Organic & Biomolecular Chemistry

Dynamic Article Links

Cite this: *Org. Biomol. Chem.*, 2011, **9**, 5573

www.rsc.org/obc

PAPER

Thermal decay of TEMPO in acidic media *via* an *N*-oxoammonium salt intermediate†

Yun Ma,[a] Colin Loyns,[b] Peter Price[b] and Victor Chechik*[a]

Received 25th March 2011, Accepted 12th May 2011
DOI: 10.1039/c1ob05475a

Disproportionation of TEMPO in acids leads to the formation of an *N*-oxoammonium salt, which can further decompose under thermal conditions, yielding the corresponding hydroxylamine, N_2O, CO_2 and a series of dimerisation products. Overall, acid-catalysed thermal decay of TEMPO leads to *ca.* 80% yield of hydroxylamine.

Introduction

TEMPO (2,2,6,6-tetramethylpiperidine-*N*-oxyl) and its derivatives are persistent free radicals widely used in chemistry[1–5] and biology.[6–8] In particular, the redox cycle of TEMPO including the corresponding hydroxylamine (TEMPOH) and oxoammonium cation (Scheme 1) forms the basis of many applications such as catalytic oxidation of alcohols[1,9–12] or dismutation of superoxide.[13]

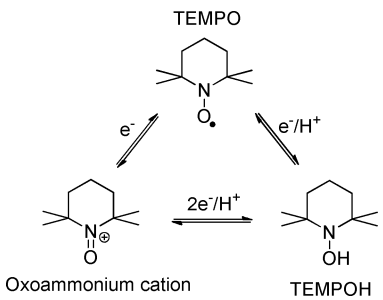

Scheme 1 Inter-conversion of TEMPO, TEMPOH and oxoammonium salt.

The reduced and oxidised forms of nitroxide radicals are also involved in the acid catalysed disproportionation reaction. Protonation of TEMPO is followed by the disproportionation, yielding TEMPOH and oxoammonium cation (Scheme 2).[14–15] The forward and reverse (*i.e.*, comproportionation[16]) reactions are well characterised at ambient temperature, including the measurement of activation parameters.[14]

However, some practical applications of nitroxide radicals in acidic medium (*e.g.*, mediation of living radical polymerisation of acidic monomers) require high temperature. The fate of nitroxide

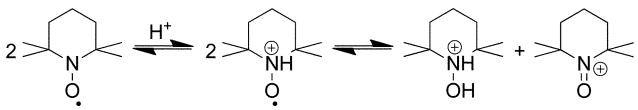

Scheme 2 Acid-catalysed disproportionation of TEMPO.

radicals in such conditions is therefore important; however literature data on thermal decomposition of nitroxides are scarce even for neutral media. Thermal decomposition of 4-oxo-TEMPO was reported by Murayama and co-workers.[17–18] It was suggested that the presence of the carbonyl group makes the 3- and 5-hydrogen atoms of 4-oxo-TEMPO more reactive, hence a self-reaction at 110 °C leads to the corresponding hydroxylamine and a nitroso-compound, which eventually yields nitric oxide (NO) and phorone (Scheme 3). Alternatively, the enol form of the hydroxylamine can be oxidised to the radical cation *via* single electron transfer (SET) followed by dimerisation (Scheme 3).[19]

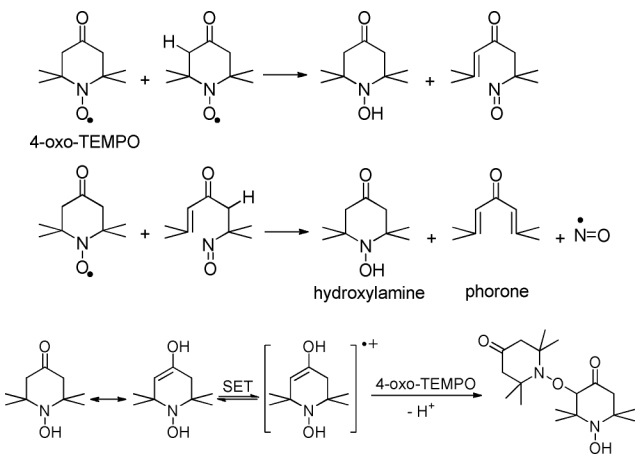

Scheme 3 Thermal decomposition and dimerisation of 4-oxo-TEMPO.

However, these reactions depend on the keto–enol tautomerism. TEMPO lacking the 4-keto group was reported[17] to be stable under the same conditions. For instance, TEMPO is stable in solvents lacking H-donating capacity until at least 150 °C.[21] In H-donating

[a]*Department of Chemistry, University of York, Heslington, York, UK YO10 5DD. E-mail: victor.chechik@york.ac.uk*
[b]*Nufarm UK Limited, Wyke Lane, Wyke, Bradford, UK BD12 9EJ*

† Electronic supplementary information (ESI) available. Kinetic modelling and spectra of TEMPO disproportionation. See DOI: 10.1039/c1ob05475a

solvents, TEMPO can be reduced to form the corresponding hydroxylamine (TEMPOH) and amine (TEMPH) at temperature above 150 °C. Elimination of NO from nitroxides is observed under photolysis; this reaction leads to the formation of the corresponding diene, similar to reactions in Scheme 3.[20]

In the presence of acids, reactions of nitroxides at elevated temperatures involve disproportionation (Scheme 2). However, the thermal stability of TEMPO and oxoammonium salt has not been studied under these conditions. Here, we report a mechanistic study of TEMPO reactivity in aqueous acids at temperatures 80–100 °C.

Results and discussion

Reversibility of TEMPO disproportionation at high temperature

In order to predict the reactivity of TEMPO in acidic medium at elevated temperature, we built a kinetic model by adopting the reported activation parameters of the disproportionation reaction.[14] TEMPO decay in dilute sulfuric acid (*e.g.* 0.1 M) was then monitored by EPR spectroscopy using an oximetry fitting method.[22] Our experimental data at room temperature fit the kinetic model precisely, but significant deviations were observed for the data obtained at higher temperature (*e.g.* 80 °C). Furthermore, the disproportionation reaction is not fully reversible under these conditions. At room temperature, increasing pH of disproportionated reaction mixture to neutral values results in fast comproportionation. For instance, after disproportionation at room temperature (decay of TEMPO EPR signal is shown in Fig. 1 with crosses), the EPR signal of TEMPO can be brought back to the original intensity upon neutralisation (Fig. 1, filled circles). However, we found that after the heating in acid at 80 °C, TEMPO cannot be recovered by neutralisation (Fig. 1, open circles).

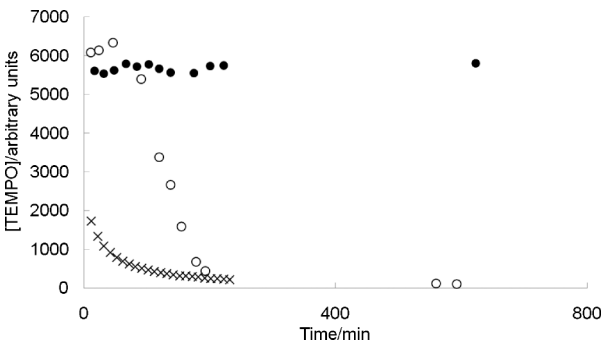

Fig. 1 EPR signal intensity of a solution of 6.4×10^{-3} M TEMPO in 1 M H_2SO_4 after neutralisation to pH = 7 at room temperature (filled circles) and 80 °C (open circles). Crosses show EPR intensity of the reaction mixture at room temperature prior to neutralisation.

Due to the high stability of TEMPO at temperatures below 100 °C,[21] these observations suggest that incomplete reversibility of TEMPO disproportionation is due to degradation of one of the disproportionation products, TEMPOH or oxoammonium salt. For instance, TEMPOH can be readily oxidised. We found, however, that under acidic conditions, protonated TEMPOH (pK_a = 6.6) has markedly high stability, showing no decomposition/oxidation at 100 °C within the time scale used in this study. In contrast, the oxoammonium salt decays rapidly at 100 °C; the decay can be monitored by the disappearance of the UV peak at 476 nm (Fig. 2). The decay fits 1st order kinetics well; the rate constant for reaction in water at 100 °C was determined as 0.120 ± 0.008 min^{-1}. The thermal decomposition of oxoammonium salt is not acid catalysed, as the reaction proceeds with a similar rate in the pH range from –0.3 to 5. The reaction does not depend on the presence of oxygen and light. We conclude therefore that stability of TEMPO in acidic solutions at high temperature is determined by the decomposition of oxoammonium salt.

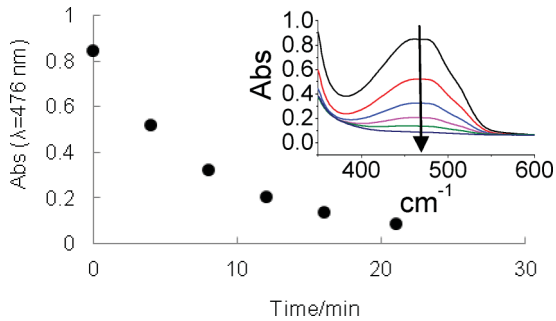

Fig. 2 Decomposition of 0.037 M oxoammonium chloride in 0.05 M H_2SO_4 at 100 °C monitored by UV-*vis* spectroscopy. Insert: Disappearance of the UV band at 476 nm over 21 min.

Oxoammonium salt as an intermediate in TEMPO decomposition

The rapid electron transfer between TEMPO and oxoammonium cation can very significantly broaden the NMR spectra which complicates product analysis of the oxoammonium salt decomposition by NMR spectroscopy. Hence, phenylhydrazine was added to the reaction mixture at different reaction times to reduce paramagnetic intermediates (and other oxidising species including unreacted oxoammonium salt). A controlled amount of phenylhydrazine was also used as an internal reference to quantify the reaction product. Interestingly, as determined by NMR spectroscopy, TEMPOH was the only component with substantial concentration after the decomposition of oxoammonium salt (*i.e.*, after complete disappearance of the UV band of oxoammonium salt). The yield of TEMPOH from decomposition of an aqueous solution of oxoammonium salt at 80 °C was estimated to be *ca.* 60%. Similarly, TEMPO decay in 0.1 M sulfuric acid at 80 °C consistently gave *ca.* 80% yield of TEMPOH. This unexpectedly clean conversion leaves only trace amounts of other products in the NMR spectra. MS spectra of the reaction mixture also revealed TEMPOH as the major product.

The main product of oxoammonium salt decomposition (and TEMPO degradation in aqueous acid) is thus the corresponding hydroxylamine TEMPOH. Since TEMPOH is a two-electron reduction product of oxoammonium salt, the reaction mixture must contain oxidation product(s) probably resulting from multiple electron transfers per molecule. It is also possible that the reaction leads to a diversity of products with low concentration. Several possible mechanisms can be proposed to explain the decomposition of oxoammonium salt. For instance, it was suggested[23] that oxidation of H_2O by oxoammonium salt leads to the formation of hydroxyl radical and TEMPO. In acid, TEMPO would disproportionate to form additional hydroxylamine and

oxoammonium salt. As a result, this mechanism would lead to the accumulation of hydroxylamine in the product.

However, this mechanism is unlikely to be correct. Firstly, oxoammonium salt decomposition was also observed in anhydrous conditions. This suggests that thermal decomposition of oxoammonium salt does not depend on the presence of H_2O. Secondly, the redox potentials of reactions (1)[24] and (2)[25] (Scheme 4) suggest that oxidation of water (to hydroxyl radical) by oxoammonium cation is physically impossible. Therefore, oxidation of water was ruled out as a possible reaction pathway.

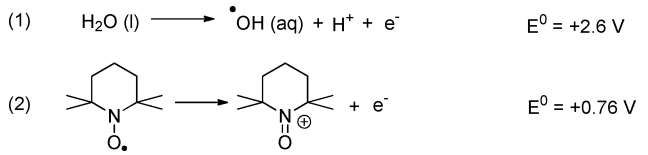

Scheme 4 Oxidation of H_2O by oxoammonium salt and the corresponding redox potentials.

Alternatively, ring opening of oxoammonium salt (Scheme 5) could lead to a carbocation which would further decompose to a series of products. Several observations favour the ring-opening route. Careful analysis of the oxoammonium salt decomposition mixture revealed some minor components that can be associated with the ring-opening process. For instance, a small amount of nitrate (*ca.* 4%) which could result from oxidation of the nitroso derivative was detected using ion-exchange chromatography. Thermal decomposition of oxoammonium salt in H_2O leads to the formation of a minor species with a UV band at 670 nm, which slowly diminishes in the presence of acid (Fig. 3). This is consistent with the $n_N \rightarrow \pi^*$ transition of C-nitroso monomers which could form *via* ring opening of the oxoammonium cation.[26] These observations are thus consistent with the ring-opening mechanism of oxoammonium salt decomposition. However the oxidation products were only detected in small amount, which leaves a missing piece in the mass balance.

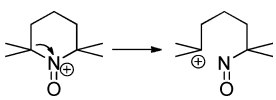

Scheme 5 Ring opening reaction of oxoammonium cation.

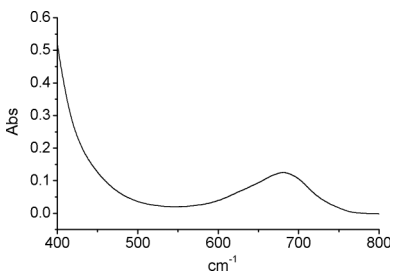

Fig. 3 UV spectrum of the reaction mixture containing 0.057 M aqueous oxoammonium salt heated at 100 °C for 20 min.

Oxoammonium salt decomposition: product analysis

In order to identify the minor reaction products, the decomposition of aqueous oxoammonium chloride was investigated on a large scale (*e.g.* several grams). As further degradation of the ring-opening product may lead to volatile molecules, the reaction was carried out in a closed system. Interestingly, formation of gas bubbles was observed during the reaction, alongside a small amount of green oily substance. The reaction products thus are distributed between the aqueous, organic and gas phases, which were analysed separately.

Analysis of the aqueous phase using NMR spectroscopy after reduction with phenylhydrazine showed TEMPOH as the only product with a yield of *ca.* 60%. In order to detect NMR silent components, the aqueous product was titrated using dilute NaOH. The resulting titration curve (Fig. 4) showed two components present in the aqueous reaction product. The first component corresponds to a strong acid with a yield of 41.4%. This strong acid could be HCl and HNO_3. Considering *ca.* 4% nitrate was detected by ion-exchange chromatography, this means ring opening of each molecule of oxoammonium chloride releases a proton, which combines with the chloride anion. The second component has pK_a 6.6 and a yield of 60.2%, which corresponds to TEMPOH. The assignment was confirmed by titration of a solution of TEMPOH in sulfuric acid with NaOH, which gave very similar pK_a value. The yield is very consistent with the yield obtained from quantitative NMR studies. Therefore, the products in the aqueous phase are TEMPOH and HNO_3/HCl.

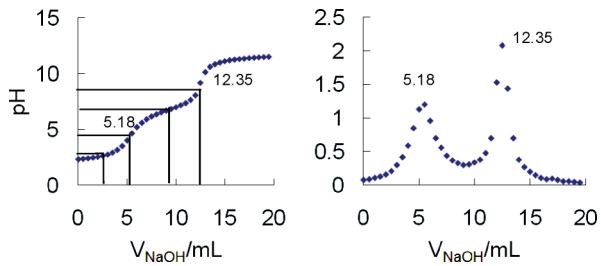

Fig. 4 Titration curve of the aqueous phase of an aqueous solution of 2.51×10^{-4} mol oxoammonium chloride heated at 100 °C for 30 min and titrated with 0.0207 M NaOH (aq). Left: titration curve. Right: 1st-derivative of the titration curve.

The gas phase product is colourless, which leaves a limited number of possible components, including CO, CO_2, NO_x and volatile hydrocarbons. A GC-FID method[27] was adopted to detect small molecule hydrocarbons, which yielded negative results. The IR spectrum of the gas product (Fig. 5) has distinctive doublets at 2212/2236 cm^{-1} and 1272/1299 cm^{-1}. These distinctive peaks are consistent with the asymmetric and symmetric stretches of nitrous oxide (N_2O).[28] In addition, the peak at *ca.* 2350 cm^{-1} suggests the presence of CO_2 in the gas product (the intensity of this peak is much greater than the background CO_2 signal). In order to estimate the amount of the gas product, we synthesised CO_2 and N_2O gases and mixed them in a 1 : 1 (v/v) ratio. The IR spectrum of the mixture (Fig. 5) is remarkably similar to the experimentally observed spectrum of the gas phase. Using these data and considering the solubility of the gases in water, the yield of CO_2 and N_2O was estimated to be 8.9% and 6.4%.

The organic phase product proved to be a complicated mixture of several components. The green colour of the organic phase suggests absorbance in the visible region of UV light. Indeed, the UV spectrum of this mixture showed the previously observed

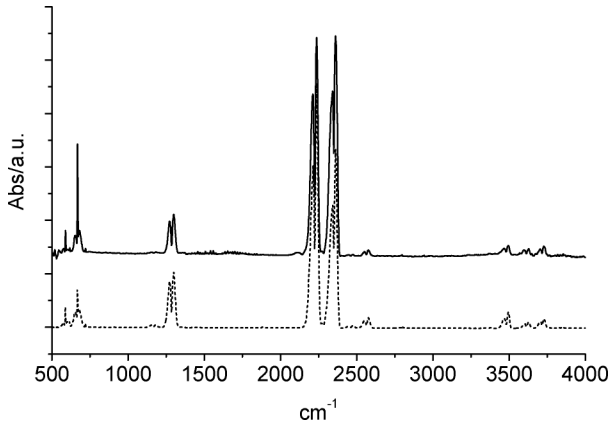

Fig. 5 Infrared spectra of the gas phase product (solid line) and a model mixture of CO_2 + N_2O (dashed line).

band at 670 nm (Fig. 3), which is consistent with the presence of a nitroso compound. TLC and GC traces revealed more than eight components in the mixture. Since the overall yield of the organic products accounts for only 3–4% (w/w) of the starting material, isolation of the components is difficult. GC-MS (EI) of the organic product did not yield exact structures for each component. Similar ions were detected for several components on the gas chromatogram. For instance, the ion at 124 *m/z* appeared as molecular ion in six peaks on the gas chromatogram. This ion can be assigned to C_9H_{16} isomers, probably dienes or cyclic alkenes. It is likely that several isomers of this compound are present in the organic phase.

In order to detect less stable products, the organic mixture was also analysed using MS (ESI) without chromatographic separation. The resulting mass spectrum provided rich information on the reaction products and indication of the reaction mechanism. The ions at 280, 298 and 327 could correspond to a series of dimerisation products (suggested structures are shown in Fig. 6). The compound with *m/z* 327 is consistent with a nitroso derivative. We note that a *C*-nitroso compound was earlier identified by the UV band at 670 nm. In addition, the ion at 154 is consistent with the product of oxoammonium cation dehydrogenation. The presence of this molecule in the product indicates that dimerised products may have formed by hydrogen abstraction from oxoammonium salt followed by addition of TEMPO or another molecule.

Mechanism of TEMPO decay in acid

With the identification of the main products of the oxoammonium salt degradation, the mechanism for the overall reaction can be proposed. The major reaction products were TEMPOH, CO_2, N_2O and dimerisation products such as $C_{18}H_{33}NO$. We propose that ring-opening of oxoammonium salt leads to a carbocation followed by elimination of nitroxyl, HNO. Nitroxyl is known to quickly dimerise to hyponitrous acid, $H_2N_2O_2$, which dehydrates to form nitrous oxide, N_2O.[29–30] The carbocation formed can be deprotonated to yield isomers of 2,6-dimethylhepta-1,5-diene (C_9H_{16}). The dienes can be oxidised under strong conditions to form CO_2 and water. Since the dimerisation products in the organic phase were formed in small amounts, the dimerisation pathway probably accounts for a small proportion of the total decomposition. The hydroxylamine (reduction product) comproportionates with oxoammonium salt to form a nitroxide radical (*e.g.* TEMPO). Hydrogen abstraction from oxoammonium salt by TEMPO forms an alkyl radical on the piperidine ring, which can dimerise by reacting with another TEMPO molecule. Alternatively, both TEMPO[31–33] and oxoammonium salt[34–35] can add to the double bond on the dehydrogenated oxoammonium salt, and thus form the dimerisation products. The overall mechanism is depicted in Scheme 6.

Conclusions

In summary, thermal decomposition of TEMPO in acidic medium proceeds *via* disproportionation reaction giving stable hydroxylamine (in the protonated form) and oxoammonium salt which undergoes a ring-opening at high temperature. This is followed by elimination of HNO from the carbocation and formation of isomers of C_9H_{16} diene. Dimerisation of HNO eventually leads to formation of N_2O gas. Oxidation of the dienes by oxoammonium salt leads to TEMPOH, CO_2 and trace amount of other products. The main product of this reaction is TEMPOH with *ca.* 80% yield.

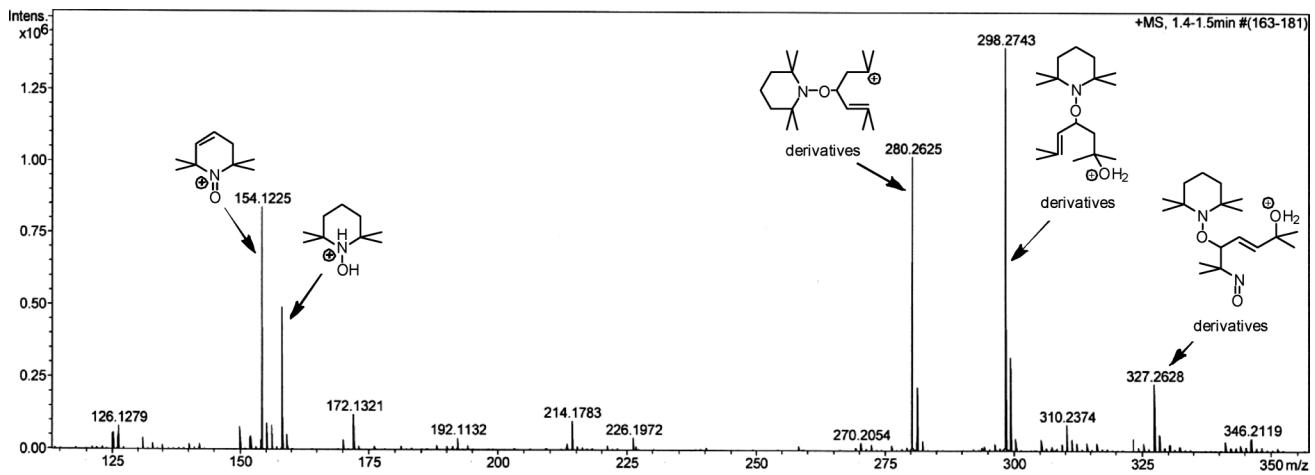

Fig. 6 Mass spectrum (+ESI) of the organic mixture (in $CHCl_3$).

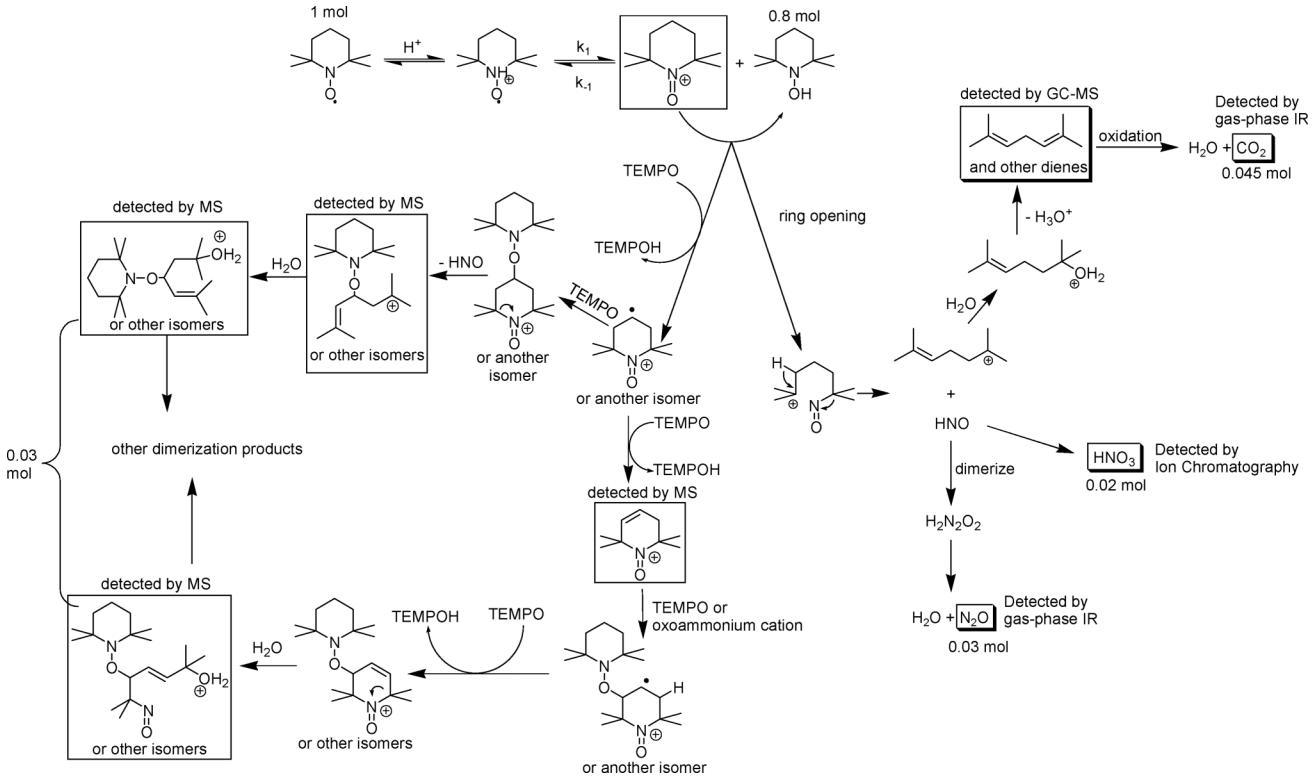

Scheme 6 Proposed mechanism of TEMPO decay at high temperature.

Experimental

Chemicals and materials

All chemicals were purchased from Sigma–Aldrich and used as received without further purification unless stated otherwise. TEMPO oxoammonium chloride was obtained from Nufarm UK Ltd.

Monitoring TEMPO decay by EPR spectroscopy

Typically a 5×10^{-4} M TEMPO in H_2SO_4 solution (*e.g.* 0.1 M H_2SO_4) was freshly prepared. Around 70 μL of this solution was transferred to a glass Pasteur pipette, with the bottom end flame sealed. The top end was sealed with lab film to prevent solvent evaporation. The glass pipette was then placed in the EPR cavity and EPR measurements were undertaken at a desired temperature (*e.g.* 80 °C) using a variable temperature setup. Typical EPR parameters were: modulation amplitude 0.5 G, microwave power 1.00 mW, acquisition time 160 s.

Monitoring oxoammonium salt decomposition by UV-*vis* spectroscopy

A solution of oxoammonium chloride (0.037 M oxoammonium salt in 0.1 M H_2SO_4) was heated at the desired temperature (*e.g.* 100 °C). At different reaction times, aliquots of the reaction mixture were taken and the UV-*vis* spectra were recorded on a double beam Hitachi U3000 spectrophotometer.

MS and GC-MS

Mass spectra were recorded on a Bruker micro-TOF spectrometer equipped with LCQ ion trap with the indicated ion sources. Gas Chromatography was performed on a VARIAN CP-3800 Gas chromatograph prior to MS analysis where indicated. The GC column used was a Zebron ZB-5HT inferno column. The temperature program was held at 60 °C for 2 min, then ramped at 5 °C min^{-1} from 60 to 350 °C followed by an isothermal period of 10 min at 350 °C. Helium was used as carrier gas at a flow rate of 2.2 ml min^{-1}. EI (70 eV) was operated at 10^{-1} unit mass resolution. ESI was operated in positive ion mode with a digital resolution of 10^{-4} unit mass.

Gas phase IR

Infra-red spectra were recorded on a JASCO FT/IR-400 spectrometer. For the gas phase IR measurements, gas samples were generated as follows. The reaction flask was charged with the reaction mixture, then degassed using freeze–pump–thaw method and re-filled with N_2. Gas formation was estimated by the readings of an attached gas syringe. The obtained gas samples were injected into a gas-tight IR cuvette cell (KBr) for measurements.

Acknowledgements

The authors thank Nufarm UK Ltd. and the University of York (Wild Fund) for funding. Dr Marco Conte is thanked for the helpful discussions. Dr James Hopkins and Miss Shalini Punjabi are thanked for their help with the headspace analysis. Mr Gareth

Moody is thanked for the GC analysis. Angela Glossop (Nufarm) is thanked for performing the IC analysis.

Notes and references

1 A. Dijksman, A. Marino-Gonzalez, A. M. I. Payeras, I. Arends and R. A. Sheldon, *J. Am. Chem. Soc.*, 2001, **123**, 6826–6833.
2 P. P. Borbat, A. J. Costa-Filho, K. A. Earle, J. K. Moscicki and J. H. Freed, *Science*, 2001, **291**, 266–269.
3 M. Pouliot, P. Renaud, K. Schenk, A. Studer and T. Vogler, *Angew. Chem., Int. Ed.*, 2009, **48**, 6037–6040.
4 M. Z. Zhao, J. Li, E. Mano, Z. G. Song, D. M. Tschaen, E. J. J. Grabowski and P. J. Reider, *J. Org. Chem.*, 1999, **64**, 2564–2566.
5 M. S. Maji, T. Pfeifer and A. Studer, *Angew. Chem., Int. Ed.*, 2008, **47**, 9547–9550.
6 S. M. Vaz and O. Augusto, *Proc. Natl. Acad. Sci. U. S. A.*, 2008, **105**, 8191–8196.
7 P. J. Wright and A. M. English, *J. Am. Chem. Soc.*, 2003, **125**, 8655–8665.
8 J. Fuchs, N. Groth, T. Herrling and G. Zimmer, *Free Radical Biol. Med.*, 1997, **22**, 967–976.
9 T. Fey, H. Fischer, S. Bachmann, K. Albert and C. Bolm, *J. Org. Chem.*, 2001, **66**, 8154–8159.
10 X. Wang, R. Liu, Y. Jin and X. Liang, *Chem.–Eur. J.*, 2008, **14**, 2679–2685.
11 R. A. Sheldon and I. Arends, *Adv. Synth. Catal.*, 2004, **346**, 1051–1071.
12 A. E. J. Denooy, A. C. Besemer and H. Vanbekkum, *Tetrahedron*, 1995, **51**, 8023–8032.
13 A. Samuni, S. Goldstein, A. Russo, J. B. Mitchell, M. C. Krishna and P. Neta, *J. Am. Chem. Soc.*, 2002, **124**, 8719–8724.
14 V. A. Golubev, V. D. Sen, I. V. Kulyk and A. L. Aleksandrov, *Bull. Acad. Sci. USSR, Div. Chem. Sci. (Engl. Transl.)*, 1975, **24**, 2119–2126.
15 V. D. Sen and V. a. Golubev, *J. Phys. Org. Chem.*, 2009, **22**, 138–143.
16 A. Israeli, M. Patt, M. Oron, A. Samuni, R. Kohen and S. Goldstein, *Free Radical Biol. Med.*, 2005, **38**, 317–324.
17 K. Murayama and T. Yoshioka, *Bull. Chem. Soc. Jpn.*, 1969, **42**, 2307–2309.
18 T. Yoshioka, S. Higashid, S. Morimura and K. Murayama, *Bull. Chem. Soc. Jpn.*, 1971, **44**, 2207.
19 A. Nilsen and R. Braslau, *J. Polym. Sci., Part A: Polym. Chem.*, 2006, **44**, 697–717.
20 J. F. W. Keana and F. Baitis, *Tetrahedron Lett.*, 1968, **9**, 365.
21 M. V. Ciriano, H. G. Korth and W. B. V. Scheppingen, *J. Am. Chem. Soc.*, 1999, **121**, 6375–6381.
22 M. Conte, Y. Ma, C. Loyns, P. Price, D. Rippon and V. Chechik, *Org. Biomol. Chem.*, 2009, **7**, 2685–2687.
23 V. A. Golubev, É. G. Rozantsev and M. B. Neiman, *Bull. Acad. Sci. USSR, Div. Chem. Sci. (Engl. Transl.)*, 1965, **14**, 1898–1904.
24 W. H. Koppenol and J. F. Liebman, *J. Phys. Chem.*, 1984, **88**, 99–101.
25 J. L. Hodgson, M. Namazian, S. E. Bottle and M. L. Coote, *J. Phys. Chem. A*, 2007, **111**, 13595–13605.
26 Y. L. Chow, J. N. S. Tam and K. S. Pillay, *Can. J. Chem.*, 1973, **51**, 2477–2485.
27 J. R. Hopkins, A. C. Lewis and K. A. Read, *J. Environ. Monit.*, 2003, **5**, 8–13.
28 T. M. Miller and V. H. Grassian, *J. Am. Chem. Soc.*, 1995, **117**, 10969–10975.
29 M. N. Hughes and H. G. Nicklin, *J. Chem. Soc. A*, 1971, 164–168.
30 P. S. Y. Wong, J. Hyun, J. M. Fukuto, F. N. Shirota, E. G. DeMaster, D. W. Shoeman and H. T. Nagasawa, *Biochemistry*, 1998, **37**, 18129–18129.
31 F. Aldabbagh, W. K. Busfield, I. D. Jenkins and S. H. Thang, *Tetrahedron Lett.*, 2000, **41**, 3673–3676.
32 J. E. Babiarz, G. T. Cunkle, A. D. DeBellis, D. Eveland, S. D. Pastor and S. P. Shum, *J. Org. Chem.*, 2002, **67**, 6831–6834.
33 A. D. Allen, B. Cheng, M. H. Fenwick, W.-w. Huang, S. Missiha, D. Tahmassebi and T. T. Tidwell, *Org. Lett.*, 1999, **1**, 693–696.
34 P. P. Pradhan, J. M. Bobbitt and W. F. Bailey, *Org. Lett.*, 2006, **8**, 5485–5487.
35 K. M. Church, L. M. Holloway, R. C. Matley and R. J. Brower, *Nucleosides, Nucleotides Nucleic Acids*, 2004, **23**, 1723–1738.

